Electrically Small Antenna with Broadside and Monopole-Like Beam Reconfigurability

Ming-Chun Tang[1], Yingjie Chen[1], Xiaoming Chen[1], Richard W. Ziolkowski[2]
[1]: School of Microelectronics and Communication Engineering, Chongqing University, Chongqing, China,
tangmingchun@cqu.edu.cn
[2]: University of Technology Sydney, Global Big Data Technologies Centre, Ultimo NSW 2007, Australia,
Richard. ziolkowski@uts.edu.au

***Abstract*—An electrically small antenna (ESA) with broadside and monopole-like beam reconfigurability is presented. It consists of an electric monopole radiator and a magnetic radiator which are systematically placed orthogonal to the ground. By controlling the PIN diodes integrated into the feed structure, broadside and monopole-like beams can be switched dynamically. The broadside beam is generated by the capacitively loaded loop (CLL) near-field resonant parasitic (NFRP) element and the monopole-like beam is formed by the electric monopole. The simulated results indicate that the antenna is impedance matched within an overlapping operational fractional bandwidth of 2.5% even though it is electrically small with *ka*=0.69. The realized gain value at boresight is 7.1 dBi for the broadside beam and the null depth is over -30 dBi for the monopole-like beam, respectively. The proposed antenna is ideal for application to GPS systems that require anti-interference performance characteristics.**

***Keywords*—Anti-interference, electrically small antenna, null depth, beam reconfigurability.**

I. INTRODUCTION

Pattern-reconfigurable antennas have recently drawn much attention due to their advantages of being able to enlarge channel volumes and to enable high anti-interference capabilities for wireless communication systems. They have been utilized in MIMO networks and satellite communications to improve system performance and to satisfy the requirements of dynamic space applications [1]. One notable set of pattern-reconfigurable antennas are those with switchable broadside and monopole-like radiation patterns. They are widely used in radar systems due to their attractive anti-interference and detection performance. They can contend with electronic jamming by changing the null position of their patterns and pointing their main beams toward desired directions, thus saving substantial electromagnetic power [2].

A variety of aforementioned antennas have been reported recently [2]-[8]. One approach is to excite different modes (e.g., TM_{10} and monopole modes) on one single radiator using switches in multi-port feed networks [2],[3] or by using reconfigurable feed networks [4]-[6]. A second approach is to utilize two-element antennas, e.g. Vivaldi antennas [7] through in-phase and out-of-phase dual-port excitation mechanisms. A third approach is based on antenna arrays. The radiation patterns are reconfigured by changing the phase differences between their radiating elements [8]. Nevertheless, all of these reported designs have large electrical sizes that are a hindrance for their wide spread use in space-limited platform applications. Thus, it is highly desirable to achieve an electrically small antenna (ESA) with broadside and monopole-like radiation patterns.

A reconfigurable ESA with broadside and monopole-like beams is reported in this paper. The proposed ESA systematically combines two orthogonally oriented radiators. One is an electric monopole element and the other is a magnetic dipole element. This architecture leads to an efficient system with an electrically small size (*ka*=0.69) that has a high-level null depth in its monopole-like beam. By controlling the states of the PIN diodes integrated into the feed structure, either radiator can be individually excited. Consequently, the system is capable of generating broadside and monopole-like beams that can be dynamically switched.

II. DESIGN OF THE RECONFIGURABLE ESA

The geometry of the proposed reconfigurable ESA is presented in Fig. 1. The corresponding optimized design parameters are given in Table I. The antenna consists of two radiators that are printed on two orthogonally oriented semi-circular substrates, labeled as Sub_2 and Sub_3, placed on and orthogonal to a circular substrate, Sub_1, that lies on a circular ground plane. One radiator is an electric monopole. The second is a magnetic radiator that is a variation of the protractor antenna [9]. These two radiators are fed by a reconfigurable structure that is printed on Sub_1. All of the substrates are Rogers 4350b, whose relative dielectric constant $\varepsilon_r = 3.48$, and loss tangent $\tan\delta = 0.0037$. They have the same thickness, $h_3 = 0.508$ mm, and radius $R_2 = 21.0$ mm. A large circular copper disc acts as the ground plane and as a reflector. It has a thickness $h_5 = 1.0$ mm and a radius $R_1 = 96.0$ mm. The feedline is connected to the center conductor of a 50-Ω coaxial cable via a hole cut through the copper ground plane. The composition of the radiating elements is copper; they are 0.017 mm thick.

As shown in Fig. 1(b), the magnetic ESA consists of two symmetrical strips and a capacitively loaded loop (CLL) near-field resonant parasitic (NFRP) element. One strip is connected to the feed structure and acts as the driven element. The other is a parasitic strip that is positioned symmetrically

with respect to the center of the outer semi-circle of the CLL. It was introduced to the original protractor design to guarantee a relatively symmetrical radiation pattern. The CLL element is etched on the other side of the Sub_2. When this magnetic ESA is excited, a broadside radiation pattern is generated.

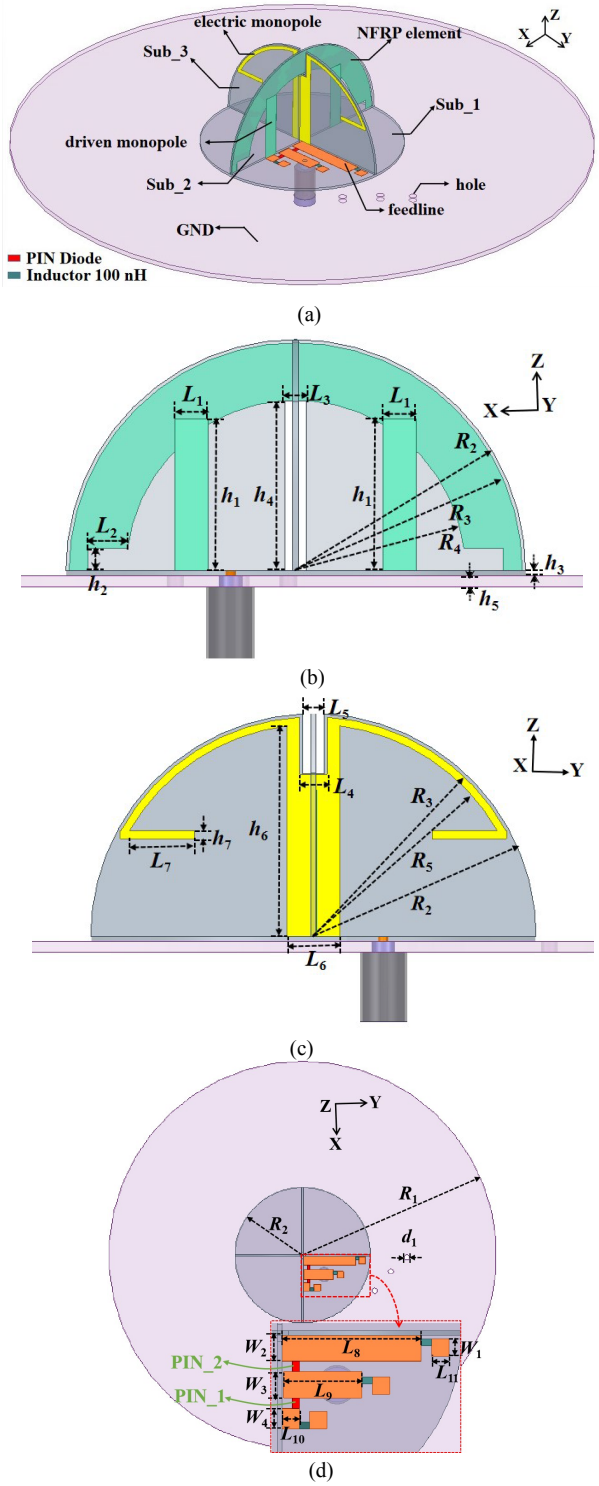

Fig. 1. Geometry of the proposed reconfigurable ESA. (a) 3D view. (b) x-z plane. (c) y-z plane. (d) x-y plane.

As shown in Fig. 1(c), the electric monopole is an Egyptian-axe shaped antenna that is printed on Sub_3. It too is directly connected to the feed structure. When the electrical monopole is excited, a deep null is achieved at boresight. Note that there are two rectangular slits etched at the lower ends of the CLL element, as well as horizontal arms attached to the monopole element. These features are introduced to fine tune the impedance matching.

TABLE II. OPTIMIZED DIMENSIONS OF THE RECONFIGURABLE ANTENNA (IN MILLIMETERS)

h_1=13.8	h_2=2	h_3=0.508	h_4=15.4	h_5=1
h_6=20	h_7=0.8	L_1=3	L_2=4.5	L_3=2
L_4 = 2.6	L_5=2	L_6=5	L_7=7	L_8=16
L_9=9	L_{10}=2	L_{11}=2	W_1=2	W_2=3
W_3=3	W_4=2.3	R_1=96	R_2=21	R_3=20.7
R_4=15.5	R_5=20	d_1=1.6	null	

The reconfigurable feed structure is accomplished using only two PIN diodes. Their layout is shown in Fig. 1(d). Both of the PIN diodes, according to their datasheet, serve as 1.5-Ω resistors in their ON state and as 0.15 pF capacitors in their OFF state. There are three Murata 100 nH inductors introduced into the feed structure to prevent any RF signals from entering the bias network. Three small holes, each with a 0.8 mm radius, are drilled in the ground disc (x-y plane). They are used to provide the routing of three dc wires to reach and be connected to the contact pads for the inductors from below the ground disc. The feed structure is configured to provide two pathways to control the ON/OFF state of the PIN diodes. State 1 represents when the diode PIN_1 is on and the diode PIN_2 is off. The CLL NFRP element is excited in this State 1 to attain the broadside beam. On the other hand, State 2 represents when PIN_1 is off and PIN_2 is on. The electric monopole is excited in this State 2 and the monopole-like beam is attained. Table II provides the relationship between the states of the PIN diodes and the two radiation states of the ESA.

TABLE I. THE STATE OF THE PIN DIODES AND THE DIFFERENT RADIATION STATES OF THE RECONFIGURABLE ANTENNA.

State	*PIN_1*	*PIN_2*	*Beam*
1	ON	OFF	Broadside
2	OFF	ON	Monopole-Like

III. SIMULATION RESULTS

All of the numerical simulations reported herein were performed using the frequency-domain, finite-element-based ANSYS/ANSOFT High-Frequency Structure Simulator (HFSS) version 18.0. Fig. 2 displays the simulated reflection coefficients together with the realized gain values over the operational band of the two states of the reconfigurable ESA. As shown in Fig. 2(a), the antenna resonates at the same frequency point, 1.57 GHz, when either one of the two states is operational. The overlapping -10 dB impedance bandwidth is from 1.55 to 1.59 GHz, which corresponds to a

fractional bandwidth of 2.5%. As illustrated in Fig. 2(b), the peak realized gain value at boresight in State 1 is 7.1 dBi, while its value in State 2 is -31.7 dBi. Thus, the gain difference between the two states at boresight is over 38 dBi. Note that the high radiation efficiency is quite high, >85%, over the entire operational bandwidth. This is achieved for both states even though the total electric size is only ka=0.69.

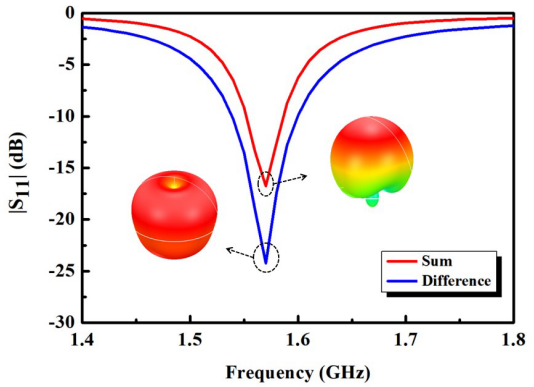

(a)

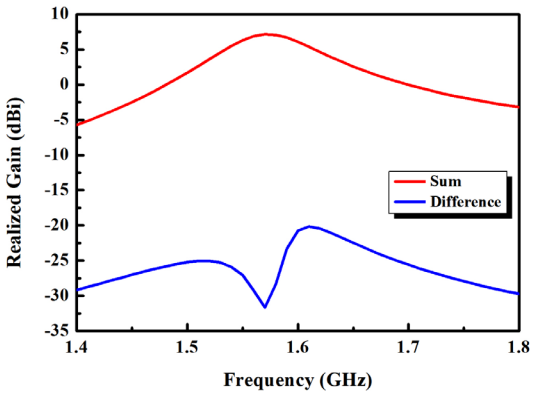

(b)

Fig. 2. Simulated $|S_{11}|$ and realized gain of broadside and monopole-like radiation patterns states. (a) $|S_{11}|$ values. (b) Realized gain at boresight values.

The simulated normalized radiation patterns at the resonant frequency 1.57 GHz of the two states are given in Fig. 3. These results demonstrate that the reconfigurable ESA exhibits excellent broadside and monopole-like radiation patterns with very low cross-polarization of the two beams at boresight. It is noted that the pattern of the monopole element has a dipole form because of the finite radius of the ground disc and the overall compact size of the entire system. This feature is emphasized with the choice to call it "monopole-like".

IV. Conclusion

A reconfigurable ESA that generates broadside and monopole-like beams was presented. The overall size is only ka = 0.69. By controlling the states of two PIN diodes, broadside and monopole-like radiation patterns are dynamically achieved. The antenna exhibits a 2.5% overlapped fractional bandwidth centered at 1.57 GHz. Moreover, relatively high radiation efficiency (RE > 85%), and symmetrical, stable, and uniform radiation patterns were achieved. The gain difference at boresight between the two states is over 38 dBi. The developed reconfigurable ESA is very suitable for GPS L1 band applications that require anti-interference performance characteristics.

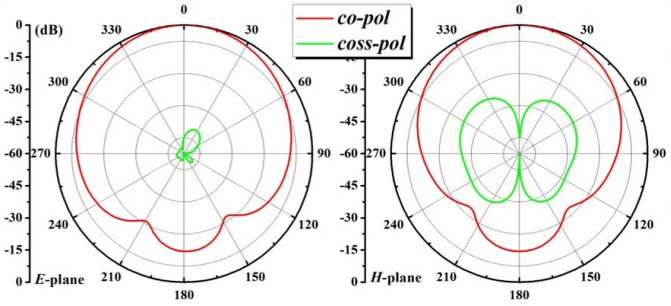

(a)

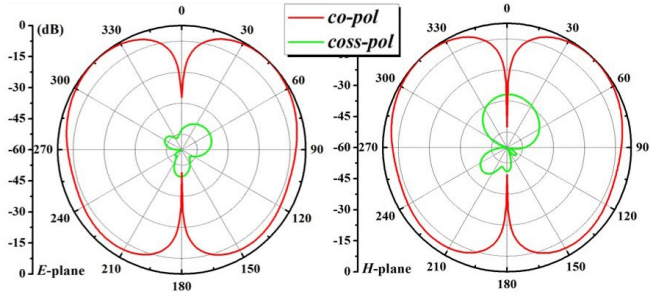

(b)

Fig. 3. Simulated radiation patterns of both broadside and monopole-like radiation patterns at the center frequency 1.57 GHz. (a) Broadside pattern. (b) monopole-like pattern.

Acknowledgment

This work was supported in part by the National Natural Science Foundation of China contract number 61922018, the Funding of the Innovative Leading Talents in Science and Technology of Chongqing contract number CSTCCXLJRC201705, in part by the Fundamental Research Funds for the Central Universities contract number 2018CDQYTX0025, in part by the Funding of the leading research talent cultivation plan of Chongqing University contract number cqu2017hbrc1A08, and in part by the Australian Research Council grant number DP160102219.

References

[1] C. G. Christodoulou, Y. Tawk, S. A. Lane, and S. R. Erwin, "Reconfigurable antennas for wireless and space applications," Proc. IEEE, vol. 100, no. 7, Jul. 2012.

[2] L. Sun, G.-X. Zhang, B.-H. Sun, W.-D. Tang, and J.-P. Yuan, "A single patch antenna with broadside and concial radiation patterns for 3G/4G pattern diversity," IEEE Antennas Wireless Propag. Lett., vol. 15, pp. 433-436, 2016.

[3] Y. B. Wen, D. Q. Yang, H. L. Zeng, M. Zou, and J. Pan, "Bandwidth enhancement of low-profile microstrip antenna for MIMO

applications," IEEE Trans. Antennas Propag., vol. 66, no. 3, pp. 1064-1075, Mar. 2018.

[4] W. Lin, H. Wong, and R. W. Ziolkowski, "Wideband pattern-reconfigurable antenna with switchable broadside and concial beams," IEEE Antennas Wireless Propag. Lett., vol. 16, pp. 2638-2641, 2017.

[5] I. Lim, and S. Lim, "Monopole-like and boresight pattern reconfifigurable antenna," IEEE Trans. Antennas Propag., vol. 61, no.12, pp. 5854-5859, Dec. 2013.

[6] X. X. Ding, Z. Q. Zhao, Y. H. Yang, Z. P. Nie, and Q. H. Liu, "A low-profile and stacked patch antenna for pattern-reconfigurable applications," IEEE Trans. Antennas Propag., vol. 67, no. 7, pp. 4830-4835, Jul. 2019.

[7] S.-A. Malakooti, M. Moosazadeh, D. C. Ranasinghe, and C. Fumeaux, "Antipodal Vivaldi antenna for sum and difference radiation patterns with reduced grating lobes," IEEE Antennas Wireless Propag. Lett., vol. 16, pp. 3139-3142, 2017.

[8] Y. J. Cheng, W. Hong, and K. Wu, "94 GHz substrate integrated monopulse antenna array," IEEE Trans. Antennas Propag., vol. 60, no. 1, pp. 121-129, Jan. 2012.

[9] P. Jin and R. W. Ziolkowski, "Multi-frequency, linear and circular polarized, metamaterial-inspired, near-field resonant parasitic antennas," IEEE Trans. Antennas Propag., vol. 59, no. 5, pp. 1446-1459, May 2011.